Electrogenerated Chemiluminescence from a Phenyleneethynylene Derivative and its Ultrasensitive Immunosensing Application Using a Nanotubular Mesoporous Pt–Ag Alloy for Signal Amplification

Mei Yan, Lei Ge, Weiqiang Gao, Jinghua Yu, Xianrang Song, Shenguang Ge, Zhiyong Jia, and Chengchao Chu*

Electrogenerated chemiluminescence (ECL) of a novel phenyleneethynylene derivatives [4,4'-(2,5-dimethoxy-1,4-phenylene)bis(ethyne-2,1-diyl) dibenzoic acid; P-acid] possessing carboxylic acid groups at the *para* positions in aqueous solutions and its first immunosensing application are studied. Nanotubular mesoporous Pt–Ag alloy nanoparticles are first used to fabricate the ECL immunosensor as a signal amplification carrier. Absorption, photoluminescence, cyclic voltammetry, scanning electron microscopy, transmission electron microscopy, and electrochemical impedance spectroscopy are used as powerful tools to characterize P-acid, Pt–Ag alloy nanoparticles, and the fabrication process of the immunosensor. P-acid exhibits two ECL peaks at –1.07 (ECL-1) and 0.64 (ECL-2) V in air-saturated pH 7.4, 0.1 M PBS containing 0.1 M KCl during the cyclic sweep between 1.51 and –2.67 V at 0.1 V s^{-1}; the ECL mechanism of these two ECL peaks is demonstrated. The electron-transfer reaction between electrochemically oxidized P-acid and tri-n-propylamine (TPrA) radical cation is also demonstrated to produce high ECL emissions and used to develop an ultrasensitive ECL immunosensor. In addition, a Pt–Ag alloy nanoparticles amplification carrier for protein ECL analysis is applied for improvement of the detection sensitivity. Thus, this ECL immunosensor exhibits high sensitivity, good reproducibility, rapid response, and long-term stability.

1. Introduction

Oligo(phenyleneethynylene)s (OPEs) are an interesting class of rigid rod π-conjugate oligomers which maintain p-electron conjugation at any degree of rotation of phenyl rings; they are drawing a great deal of attention for electronic communication in molecular electronic devices.[1–3] The tunable and versatile optical properties and semiconducting properties of OPEs both in solution and in the solid state[4] have made them very useful in chemical sensors[5–11] and so forth. Oligo(phenyleneethynylene)s are complementary and in some cases may be superior to the existing fluorophores.[9] Further exploration of their superior emitting properties by different methods is of great importance.

Electrogenerated chemiluminescence (ECL), the generation of an optical emitting triggered by an electrochemical reaction, has the inherent advantages of versatility, sensitivity, selectivity, simplified optical setup, good temporal and spatial control, and wide linear range for clinical tests and biomolecules detection.[12] Although many ECL systems have been employed for ECL analysis – such as various organometallic complexes[13–17] or polymers,[18] luminal,[19–21] semiconductor nanocrystal,[22–25] and organic[26] compounds – reports concerning ECL analysis through π-conjugate oligomers are relatively scarce.[27] In this work, a novel phenyleneethynylene derivatives possessing carboxylic acid groups at the *para* positions [4,4′-(2,5-dimethoxy-1,4-phenylene) bis(ethyne-2,1-diyl)dibenzoic acid; P-acid] was synthesized using a Heck–Cassar–Sonagashira–Hagihara cross-coupling reaction and was demonstrated to have the ability of ECL in the presence of dissolved oxygen or tri-n-propylamine (TPrA).

Finally, to demonstrated the application of P-acid in analytical chemistry, a ultrasensitive ECL immunosensor for carcinoembryonic antigen (CEA) based on this excellent P-acid-TPrA ECL system was demonstrated through signal amplification with the aid of novel nanotubular mesoporous Pt–Ag alloy nanoparticles, for the first time.[28] Nanotubular mesoporous alloy nanoparticles are of considerable interest as protein immobilization carriers[29] due to their hollow porous nanostructures having the advantage of highly accessible surface areas, and their rich

Prof. M. Yan, L. Ge, W. Gao, Prof. J. H. Yu, S. G. Ge, Z. Y. Jia, C. C. Chu
Key Laboratory of Chemical Sensing & Analysis in Universities of Shandong
School of Chemistry and Chemical Engineering
University of Jinan
250022, P. R. China
E-mail: ujn.yujh@gmail.com
Prof. X. R. Song
Cancer Research Center
Shandong Tumor Hospital
250117, P. R. China

DOI: 10.1002/adfm.201200544

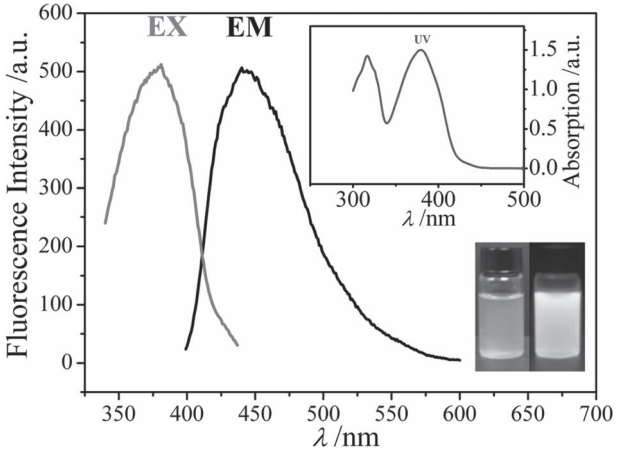

Figure 1. UV-visible absorption and emission spectra of P-acid recorded in aqueous solution at 293 K. The concentration of P-acid is 40 μM. The inset shows photographs of the P-acid in aqueous solution under visible light (left) and 365 nm UV light (right).

surface chemistry allowing further vast functionalization of P-acid for ultrasensitive and multilabeling signal amplification. The results indicate that this novel ECL system possesses great potential in the application of various ECL sensors.

2. Results and Discussion

2.1. Absorption and Emission

The absorption spectrum of as-prepared P-acid in aqueous solution is shown in **Figure 1**. The spectrum has a shorter wavelength band with a maximum around 315 nm, with partially resolved vibronic features, and a long wavelength band with a maximum around 367 nm of almost the same intensity. The prepared P-acid exhibited a blue color under ultraviolet radiation (λ = 365 nm) (Figure 1). The fluorescence spectrum of P-acid is shown in Figure 1; excitation into the long absorption band produces room-temperature photoluminescence and the maximum fluorescent emission was obtained at the wavelength of 481 nm, indicated that the P-acid molecule has favorable properties for fluorescence. Moreover, the small energy difference between excitation and emission spectra indicates the existence of a π-conjugated structure.

2.2. Electrochemical and ECL Behaviors of P-acid

Figure 2 shows the cyclic voltammetry and ECL curves of the P-acid in PBS (0.1 M, pH 7.4) containing KCl (0.1 M). The Au working electrode in the air-saturated solution of PBS (0.1 M, pH 7.4) containing KCl (0.1 M) showed very low background current, and no light emission was observed (data not shown). In the air-saturated solution of PBS (0.1 M, pH 7.4) containing KCl (0.1 M) and 1 mM P-acid, P-acid exhibited reversible oxidation waves (1.08 and 0.81 V) and reversible reduction waves (–2.13 and –1.97 V) (Figure 2A). At the same time, two ECL peaks were observed at –1.07 V (ECL-1) and 0.64 V (ECL-2) (curve a in Figure 2B).

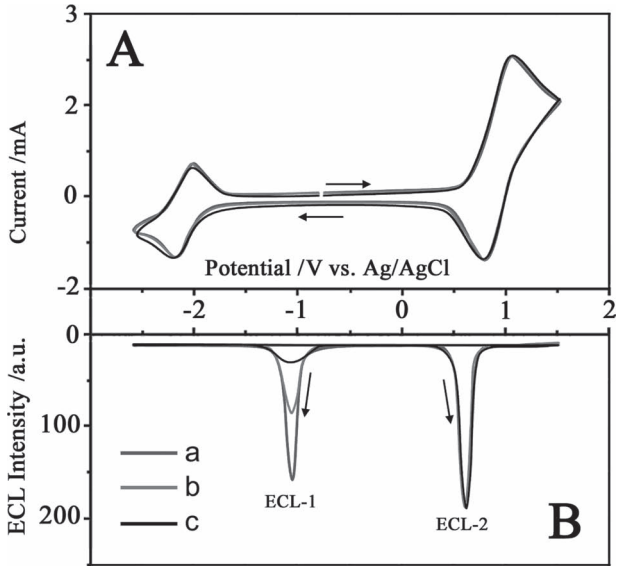

Figure 2. Cyclic voltammograms (A) and ECL curves (B) of P-acid in air-saturated 0.1 M pH 7.4 PBS containing 0.1 M KCl and 1 mM P-acid: a) as-prepared solution, b) as-prepared solution bubbled with N_2 for 25 min, and c) as-prepapred solution withthe addition of 0.1 M Na_2SO_3. The scan rate was 0.1 V s^{-1}.

As shown in Figure 2, ECL-1 should be obtained from the reaction between co-reactants and P-acid. Here, the co-reactants should be dissolved oxygen or its reduced product OOH^-.[30] When dissolved oxygen was removed from the solution by bubbling with high-purity nitrogen for 25 min, the light emission intensity of ECL-1 decreased dramatically (curve b in Figure 2B). When dissolved oxygen was further removed by adding Na_2SO_3 to the solution or bubbling high-purity nitrogen for a prolonged time, the ECL intensity further decreased (curve c in Figure 2B). Thus, dissolved oxygen or its reduced product OOH^- participated in the electrode process and ECL reactions. The ECL mechanism for ECL-1 can be demonstrated as follows. Few electrons are available in the high energy band (HOMO) of the π-conjugate phenyleneethynylene at absolute zero. However, as the temperature rises above absolute zero, there is more energy to excite electrons into the HOMO of π-conjugate phenyleneethynylene.[31] The thermally excited electrons into HOMO of π-conjugate phenyleneethynylene annihilate with the injected holes to produce the ECL.[32,33] The injection of holes into the π-conjugate phenyleneethynylene of P-acid by oxidants (dissolved oxygen or its reduced product OOH^-) increases the number of holes in the π-conjugate phenyleneethynylene and accelerates electron–hole annihilation, which results in energy release in the form of ECL emissions. Similarly, ECL-2 should be obtained from hole injection into the π-conjugate phenyleneethynylene of P-acid by the working electrode directly. When ascorbic acid, which is an effective hole scavenger,[34] was added to the solution, the light emission intensity of ECL-2 decreased dramatically (curve a in **Figure 3**) compared with ECL-2 in Figure 2B. At the same time, the oxidation peak of ascorbic acid at 0.55 V was observed (curve b in Figure 3). When holes were further scavenged by adding more ascorbic acid to the solution, the ECL intensity further decreased (curve c in Figure 3) while the oxidation peak of ascorbic acid further increased (curve d in Figure 3). Thus, the injection of holes from the working

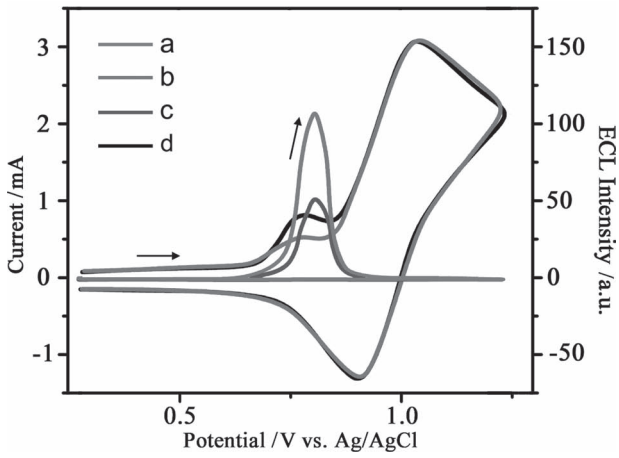

Figure 3. The anodic ECL curves and cyclic voltammograms of P-acid (1 mM) in air-saturated 0.1 M pH 7.4 PBS containing 0.1 M KCl and 0.1 mM ascorbic acid (a and b, respectively) and air-saturated 0.1 M pH 7.4 PBS containing 0.1 M KCl and 0.15 mM ascorbic acid (c and d, respectively). The scan rate was 0.1 V s^{-1}.

electrode, which annihilate the thermally excited electrons in the HOMO of the π-conjugate phenyleneethynylene of P-acid, results in energy release in the form of ECL-2 emission.

As is well-known, tri-n-propylamine (TPrA) is always used as co-reactant in the anodic $Ru(bpy)_3^{2+}$ (bpy = 2,2′-bipyridyl) ECL system.[12] In this study, as shown in **Figure 4**, upon addition of 10 mM TPrA, direct oxidation started at about 0.6 V, with an enhanced ECL emission peak at the potential of the P-acid oxidation compared with the ECL-2 in Figure 2B. With the addition of TPrA, the anodic wave for P-acid oxidation was greatly enhanced and the reduction wave disappeared compared with the cyclic voltammograms in Figure 2A. Thus, TPrA should be also a co-reactant to produce ECL emissions, and the electrochemical and ECL process can be expressed as follows according to previous studies:[12]

$$\text{P-acid-e}^- \rightarrow \text{P-acid}^+ \quad (1)$$

$$\text{TPrA-e}^- \rightarrow [\text{TPrA}]^+ \rightarrow \text{TPrA}^\bullet + \text{H}^+ \quad (2)$$

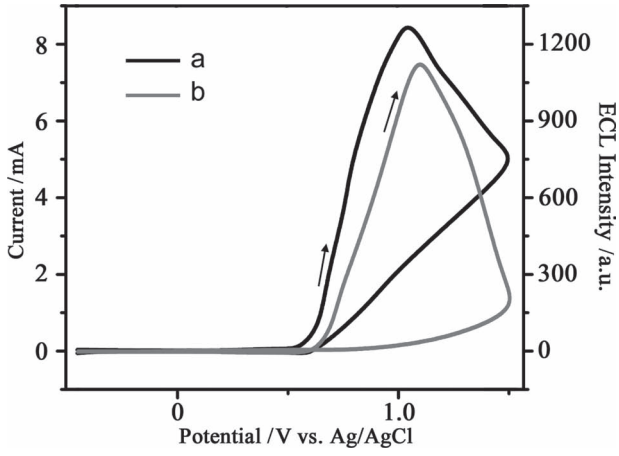

Figure 4. a) Cyclic voltammograms of P-acid (1 mM) in 0.1 M PBS (pH 7.4) containing 0.1 M KCl in the presence of 10 mM TPrA. b) The ECL signal curve recorded during the CV.

$$\text{P-acid}^+ + \text{TPrA}^\bullet \rightarrow \text{P-acid}^* + \text{products} \quad (3)$$

$$\text{P-acid}^* \rightarrow \text{P-acid} + h\nu \quad (4)$$

2.3. Characterization of Antibodies/P-acid/Pt–Ag Alloy Nanoparticles

Figure 5 illustrates the morphology of nanotubular mesoporous Pt–Ag alloy nanoparticles and P-acid/Pt–Ag alloy nanoparticles. As shown in Figure 5a and b, the tube openings on the surface reveal the formation of hollow interiors within the mesoporous configuration. The clear color contrast in the TEM image (Figure 5a) further confirms the formation of a 3D nanotubular

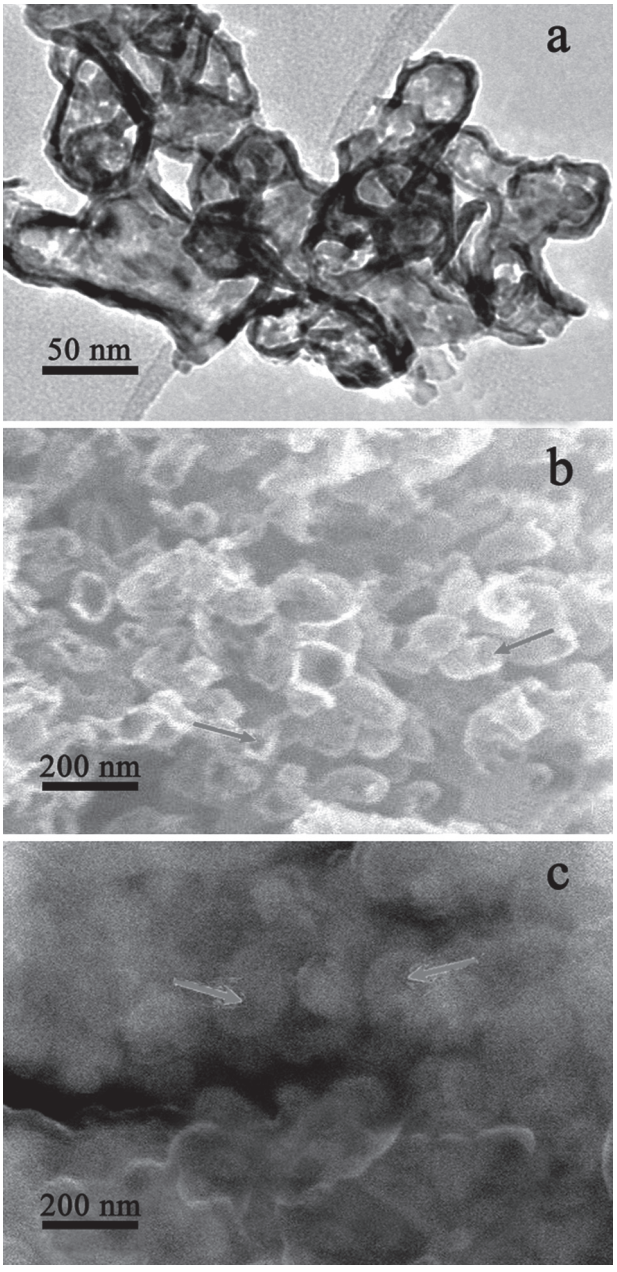

Figure 5. a) TEM and b) SEM of the nanotubular mesoporous Pt–Ag alloy nanoparticles. c) SEM of P-acid/Pt–Ag alloy nanoparticles.

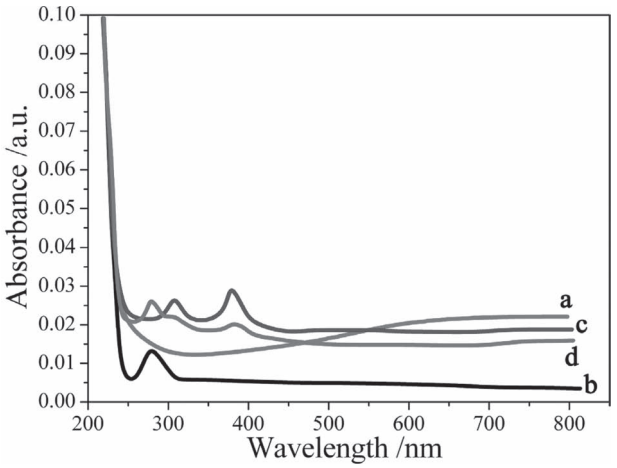

Figure 6. UV-vis spectra of a) Pt–Ag alloy nanoparticles, b) anti-CEA antibodies, c) P-acid/Pt–Ag alloy nanoparticles, and d) antibodies/P-acid/Pt–Ag alloy nanoparticles.

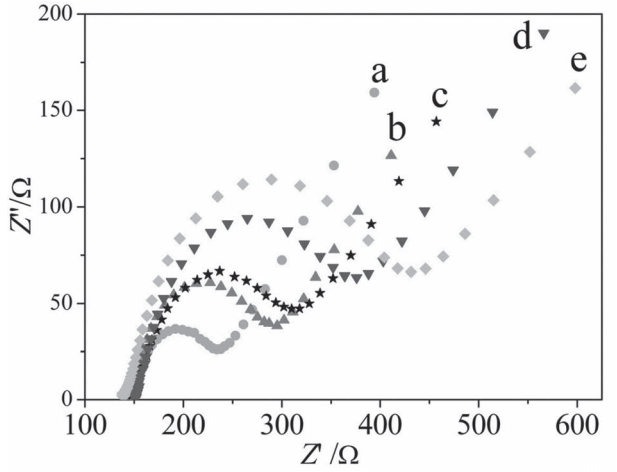

Figure 7. Electrochemical impedance spectroscopy of the electrode at different stages: a) Bare Au working electrode, b) after immobilization of capture antibodies, c) after blocking with BSA, d) after capture of CEA, and e) after the immobilization of signal antibodies. Supporting electrolyte: 10 mM PBS (2.5 mM $Fe(CN)_6^{4-/3-}$ + 0.1 M KCl, pH 7.4).

mesoporous structure with a tube diameter of 50 nm and a shell thickness of 7 nm.[28] As indicated by the red arrows in Figure 5c, P-acid could be immobilized into the nanotubular mesoporous structure of the Pt–Ag alloy nanoparticles through ethanediamine cross-linking with a slightly coarsened ligament size of 80 nm.

The antibodies/P-acid/Pt–Ag alloy nanoparticles (signal antibodies) were further characterized using UV-vis spectroscopy (**Figure 6**). According to the UV-vis spectral experiments, no absorption peak was observed for the Pt–Ag alloy nanoparticles (curve a). Two distinct adsorption peaks from P-acid were observed on the spectra of P-acid/Pt–Ag alloy nanoparticles (curve c), which may be attributed to the adsorption peaks from P-acid itself mentioned above (Figure 1). After the immobilization of antibodies, another distinct adsorption peak from the antibodies was observed on the spectra of antibodies/P-acid/Pt–Ag alloy nanoparticles (curve d), which may be attributed to the adsorption peak from the antibody itself at 282 nm (curve b).

2.4. Characterization of the Immunosensor

Electrochemical impedance spectroscopy (EIS) was an effective method to monitor the features of the modified electrode surface. The impedance spectra include a semicircular portion and a linear portion. From the EIS of the electrode at different stages (**Figure 7**), it was observed that the bare Au electrode exhibited a low electron-transfer resistance of the redox couple (curve a), which was characteristic of a diffusional process. When the capture antibodies were assembled onto the Au working electrode (curve b), access to the interfacial electron transfer was hindered, which suggests that capture antibodies were immobilized on the Au working electrode and blocked electron exchange between the redox probe and the electrode. In the case of BSA/capture antibodies/Au, the R_{et} further increased (curve c). Additionally, after the capture of CEA (curve d) and the signal antibodies (curve e), the resistance increased again, this indicated that the electrode was well-modified.

2.5. Signal Amplification using Pt–Ag Alloy Nanoparticles

The ECL response of the as-prepared ultrasensitive immunosensor was shown in **Figure 8**. As a comparison, the ECL

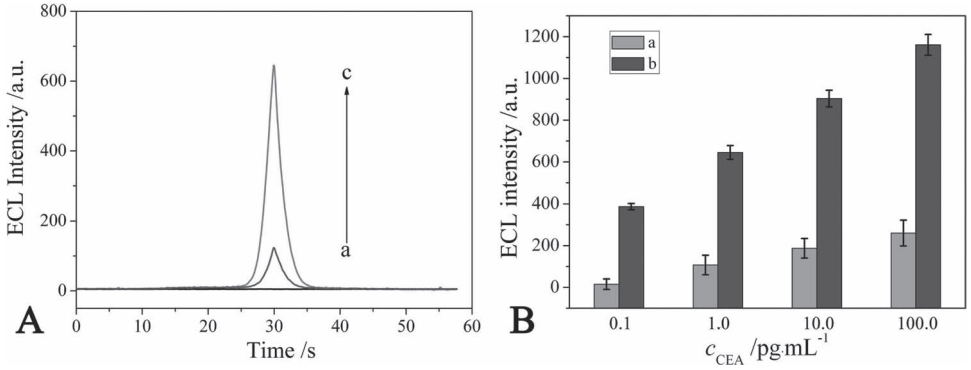

Figure 8. A) ECL response of: a)capture-antibodies-modified Au working electrode incubated with 1 pg mL^{-1} CEA, b) incubated with antibodies/P-acid labeled signal antibodies, c) incubated with antibodies/P-acid/Pt–Ag alloy nanoparticles labeled signal antibodies. B) Comparison of ECL response between antibodies/P-acid label (a) and antibodies/P-acid/Pt–Ag alloy nanoparticles label (b) at different concentrations of CEA (0.1, 1, 10, and 100 pg mL^{-1}).

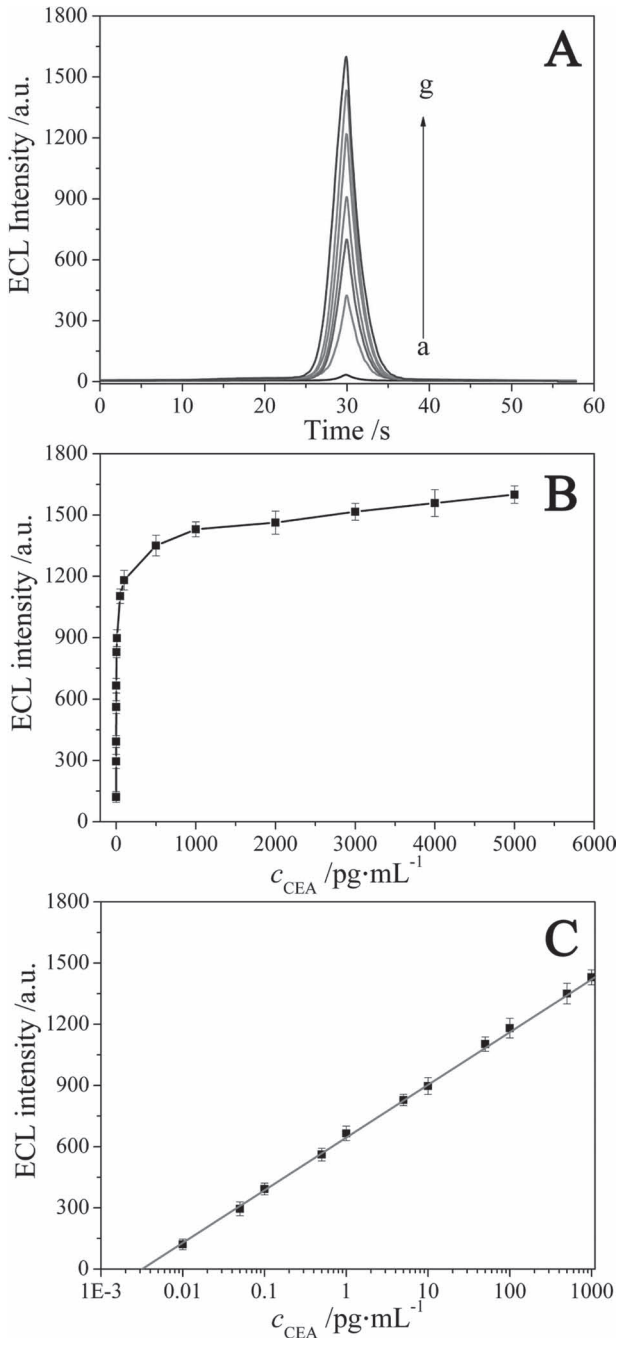

Figure 9. A) ECL signals of this immunosensor incubated with different concentrations of CEA (from bottom to top, 0 pg mL^{-1}, 0.1 pg mL^{-1}, 1 pg mL^{-1}, 10 pg mL^{-1}, 100 pg mL^{-1}, 1 ng mL^{-1}, 5 ng mL^{-1}. B) Relationship between *I* and CEA concentration each point is the average of three measurements. C) Logarithmic calibration curve for CEA.

response of antibodies/P-acid label was also investigated. Under the same conditions, the signal intensity was greatly decreased compared with the antibodies/P-acid/Pt–Ag alloy nanoparticles label at the same (Figure 8A) and different (Figure 8B) concentrations of CEA. These results indicate that the analysis sensitivity was greatly enhanced using antibodies/P-acid/Pt–Ag alloy nanoparticles as label, which was the result of a higher number of P-acid molecules loaded on the antibodies to achieve the signal amplification. Therefore, the proposed immunosensor exhibited a good analytical performance for the CEA detection and could be used for the detection of CEA in real samples.

2.6. Analytical Performance

Figure 9A showed the ECL intensity of the immunosensor in the absence (a) and presence (b–g) of different concentrations of CEA. It can be seen that the ECL intensity in the presence of CEA (b) was higher than that in the absence of CEA (a), and the ECL intensity increased gradually with increasing concentrations of CEA (b–g). The reason was that the specific binding of antigen and signal antibodies could produce the ECL reaction of P-acid and TPrA on the electrode, and thus increased the ECL intensity, which suggested that the CEA concentration could be determined by the ECL measurement of this immunosensor.

The standard calibration curve for the CEA detection is shown in Figure 9B and C. The ECL intensity increased linearly with the CEA concentration from 0.01 pg mL^{-1} to 10 ng mL^{-1} with a detection limit of 3 fg mL^{-1}. The linear fit equation is $I_1 = 644.9 + 258.3 \lg c$ (unit of c is ng mL^{-1}), with a correlation coefficient of 0.9973. According to the linear equation, we could detect trace CEA concentration quantitatively. Higher plasma CEA levels could be detected by an appropriate dilution with pH 7.4 PBS.

2.7. Precision, Reproducibility, and Stability of this ECL Immunosensor

The reproducibility of the immunosensor for CEA was investigated with intra- and inter-assay precision. The intra-assay precision of the immunosensor was evaluated by assaying one CEA level for ten replicate measurements. The inter-assay precision was estimated by determining one CEA level with ten immunosensors made at the same electrode. The intra- and inter-assay variation coefficients (CVs) obtained from 0.008 pg mL^{-1} CEA were 3.1 and 5.7%, respectively. Obviously, the inter-assay CV showed an acceptable precision and reproducibility; while the low value of intra-assay CV indicated that the immunosensor could be regenerated and used repeatedly. After the immunosensor was continuous scanned for 15 cycles (**Figure 10**), stable and high ECL signals were observed, demonstrating that this immunosensor possessed good stability and was suitable for ECL detection. When this ECL immunosensor was stored and measured at intervals of 3 d, no obvious change was observed after 2 weeks under ambient conditions or 5 weeks under dry conditions at 4°C. These results indicated that the immunosensor array has acceptable stability and suitability for storage or long-distance transport to remote regions and developing countries.

2.8. Application of the Immunosensor in Human CEA Levels

The plasma CEA levels in two samples were analyzed by using this ECL immunosensor. These two samples were first diluted

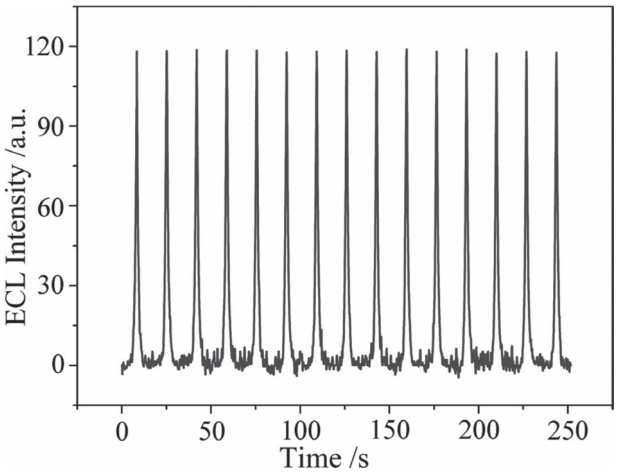

Figure 10. ECL emission from the immunosensor immobilized with sandwich immunocomplexes labeled with P-acid/Pt–Ag alloy nanoparticles in PBS (pH 7.4) containing KCl (0.1 M) under continuous cyclic voltammetry for 15 cycles. Scan rate: 0.1 V s^{-1}; scan range: 0.2 to 1.0 V.

to 8.0 and 15.0 pg mL^{-1}, respectively. According to the standard curve, the mean plasma CEA concentrations were determined to be 8.1 and 14.7 pg mL^{-1}, which were in acceptable agreement with the above results. The relative errors were 1.3% and 2.0%, respectively. Compared with the assay results (8.2 and 15.5 pg mL^{-1}) obtained by a commercially used electrochemiluminescence method at the Cancer Research Center of Shandong Tumor Hospital, the relative errors were 2.5% and 3.3%, respectively. Thus, the proposed ECL immunosensor could be satisfactorily applied to the clinical determination of CEA levels in human plasma.

3. Conclusions

Electrogenerated chemiluminescence of a novel phenyleneethynylene derivatives possessing carboxylic acid groups at the *para* positions (P-acid) in air-saturated aqueous solutions was demonstrated for the first time. Two ECL peaks were exhibited upon a total potential scan, which correspond to the same hole injection mechanisms. The first ECL peak results from hole injection from co-reactants (dissolved oxygen or its reduced product OOH^- produced at cathodic process) into the π-conjugate phenyleneethynylene of P-acid. Similarly, the second ECL peak is due to hole injection from the electrode directly. Upon an anodic potential scan, TPrA is another co-reactant to produce high ECL emission, which are obtained from the electron-transfer reaction between reducing intermediate $TPrA^{\bullet}$ and oxidized P-acid produced through an anodic process. Based on this " oxidative–reductive" ECL system, a novel ultrasensitive ECL immunosensor was demonstrated to test the application of this ECL system. This ECL sensor shows a linear response to CEA ranging from 0.01 pg mL^{-1} to 10 ng mL^{-1} with good sensitivity and reproducibility. The detection limit is 3 fg mL^{-1}. Such an ECL immunosensor also offers new opportunities for ultrasensitive detection of biomolecules at very low concentrations, and it is expected to provide new possibilities for protein diagnostics as well as for bioanalysis in general.

4. Experimental Section

Methods and Materials: Mouse monoclonal anti-CEA antibodies were purchased from Linc-Bio Science Co. Ltd. (Shanghai, China). All chemicals were of analytical grade and purchased from Sigma-Aldrich or Alfa-Aesar. Ultrapure water obtained from a Millipore water purification system (g18 MU, Milli-Q, Millipore) was used in all assays and solutions. Blocking buffer for blocking the residual reactive sites on the antibody immobilized paper was 0.1 M pH 7.4 phosphate buffer solution (PBS) containing 0.5% BSA and 0.5% casein. To minimize unspecific adsorption, 0.05% Tween-20 was spiked into 0.1 M pH 7.4 PBS as washing buffer. The clinical serum samples were from Shandong Tumor Hospital.

Synthesis of P-acid: P-acid was synthesized according to a previous protocol with major modifications;[4] the procedure is shown in **Scheme 1**.

Synthesis of **1**: To a solution of 1,4-dimethoxy benzene (2.76 g, 20 mmol) in 20 mL of acetic acid, 2 mL of water and 1 mL of concentrated H_2SO_4, KIO_4 (5.52 g, 24 mmol) and I_2 (6.09 g, 24 mmol) were added. The reaction mixture was stirred at 120°C for 24 h and then cooled to room temperature. The excess iodine was removed by the addition of sodium thiosulphate solution until the brown color of iodine disappeared. The excess H_2SO_4 was neutralized with Na_2CO_3 solution until the brisk effervescence stopped. The residue was extracted with chloroform. The white solid product (7.79 g, 69%) was separated using a silica column with hexane as eluent. IR (cm^{-1}): 3040 (phenyl ring C–H); 2959, 2932, 2832 (methyl C–H); 1605, 1508, 1474 (phenyl ring C–C); 1264, 1053 (C–O–C); 1375, 1450 (methyl C–H); 707 (phenyl ring C–C).

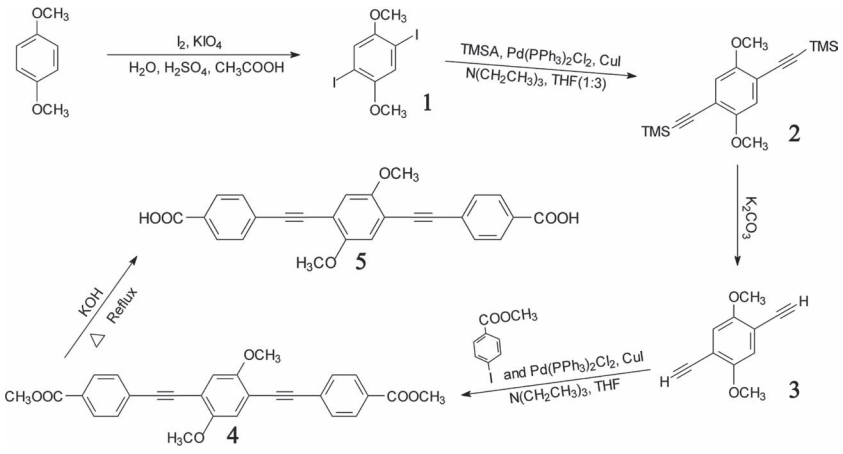

Scheme 1. Synthesis of P-acid.

Synthesis of **2**: To the solvent of triethylamine and tetrahydrofuran (THF) (1:3), compound 1 (1.17 g, 3.90 mmol), CuI (0.023 g, 0.12 mmol) and $Pd(PPh_3)_2Cl_2$ (0.020 g, 0.03mmol) in 37.72 mL of diisopropylamine, trimethylsilylacetylene (TMSA) (0.90 mL, 6.40 mmol) was slowly added. The mixture was stirred at reflux using ice-cold condensing circulation for about 3 h. The reaction mixture passed through a short celite column and further purified by column chromatography using silica column with petroleum ether/methylene chloride (4:1) as eluent to obtain white crystals of **2** (0.93 g, 72%). IR (cm^{-1}): 3045 (phenyl ring C–H); 2956, 2902, 2840 (methyl C–H); 2148 (C≡C); 1606,

1510, 1457 (phenyl ring C–C); 1260, 1049 (C–O–C); 1370, 1456 (methyl C–H); 705 (phenyl ring C–C).

Synthesis of **3**: To a solution of **2** (0.58 g) in THF (25 mL), methanol (25 mL) and K_2CO_3 (0.974 g, 7.06 mmoL) were added and the mixture stirred for 5 h. The solvent was evaporated and the residue was poured into water and extracted with chloroform. The organic layer was washed with salt-saturated solution and dried over anhydrous sodium sulphate. A yellow solid product (0.27 g, 82%) was obtained after the solvent was removed. IR (cm^{-1}): 3314 (≡C–H); 3036 (phenyl ring C–H); 2956, 2902, 2840 (methyl C–H); 2146 (C≡C); 1606, 1508, 1484 (phenyl ring C–C); 1375, 1450 (methyl C–H); 1247 (≡C–H); 1264, 1053(C–O–C); 704 (phenyl ring C–C).

Synthesis of **4**: To a solution of **3** (1.16 g, 6.24 mmol), CuI (0.118 g, 0.62 mmol), methyl 4-iodobenzoate (3.27 g, 12.48 mmol) and $Pd(PPh3)_2Cl_2$ (0.2 g, 0.29 mmol) in triethylamine and THF (1:3) was added and refluxed for 12 h. The residue was concentrated and the yellow solid product (2.21 g, 78%) purified by column chromatography over silica using methylene chloride/petroleum ether (2:1) as eluent. IR (cm^{-1}): 3008 (phenyl ring C–H); 2947, 2902, 2840 (methyl C–H); 2148 (C≡C); 1719 (C=O); 1602, 1508, 1492 (phenyl ring C–C); 1375, 1450 (methyl C–H); 1275, 1053 (C–O–C); 707 (phenyl ring C–C).

Synthesis of P-acid: To a solution of HPLC purified **4** (0.1 g) in THF (15 mL), KOH (1.0 g) and methanol (8 mL) were added and refluxed at a temperature of 70 °C for about 5 h. The reaction mixture neutralized with dilute HCl to remove excess alkali and 50 mL water was added to precipitate the product. The mixture extracted with chloroform and the combined chloroform layer was evaporated under reduced pressure to yield the yellow solid product P-acid (0.09 g, 95%). IR (cm^{-1}): 3415 (carboxyl OH); 3008 (phenyl ring C–H); 2947, 2902, 2840 (methyl C–H); 2148 (C≡C); 1719 (C=O); 1602, 1508, 1492 (phenyl ring C–C); 1375, 1450 (methyl C–H); 1275, 1053 (C–O–C); 1420, 1243 (carboxyl OH); 707 (phenyl ring C–C). ^{1}H NMR (400 MHz, DMSO, TMS) (Figure S1 in the Supporting Information): δ 13.189 (s, 2H, COOH), δ 7.976–7.996 (d, 4H, aromatic), δ 7.653–7.674 (d, 4H, aromatic), δ 7.262 (s, 2H, aromatic), δ 3.856–3.871 (s, 6H, OCH_3).

Preparation of Nanotubular Mesoporous Pt–Ag Alloy Nanoparticles: Nanotubular mesoporous Pt–Ag alloy nanoparticles were synthesized according to Xu et al.'s reported method.[28] Briefly, porous silver was fabricated by selectively dealloying Al from Ag–Al alloy nanoparticles in 1 M NaOH corrosive electrolytes at room temperature (30 °C) for 72 h. The high-surface-area nanotubular mesoporous Ag nanoparticles were used as an effective template materials for the construction of nanotubular mesoporous Pt–Ag alloy nanoparticles, which were realized via room-temperature galvanic replacement reactions with H_2PtCl_6 solutions by adding a high concentration of Cl^- (above 3 M) ions as a coordinating agent at 30 °C for 1 h.

Preparation of Antibodies/P-acid/Pt–Ag Alloy Nanoparticles (Signal Antibodies): For the immobilization of P-acid, briefly, ethylenediamine (2 mL) and nanotubular mesoporous Pt–Ag alloy nanoparticles (1 mg) were dispersed in 5 mL of ethanol by sonication for 1 h. It has been proven that amino groups can be bound strongly to Pt.[35] Then, the resulting amino group functionalized nanotubular mesoporous Pt–Ag alloy nanoparticles were washed with 5 mL buffer solution (pH 7.4) and then centrifuge separated. Then, amino group functionalized Pt–Ag alloy nanoparticles were added into the anhydrous solution of P-acid (3 mM, 5 mL) containing 6 mM *N,N'*-carbonyldiimidazole (CDI) by sonication for 2 h. CDI could react with carboxyl group or hydroxyl groups to form an active imidazole carbamate intermediate. In the presence of amino groups, a carbamate linkage is created with loss of imidazole.[36] After the activated P-acid/Pt–Ag alloy nanoparticles were thoroughly rinsed with ultrapure water, they were immediately redispersed into CEA (3 mL, 20 μg mL^{-1}) secondary antibodies solution and then incubated for 2 h to form the signal antibodies. The resulting signal antibodies were washed with buffer solution (pH 7.4) and then redispersed in 1 mL pH 7.4 PBS and stored at 4 °C before use.

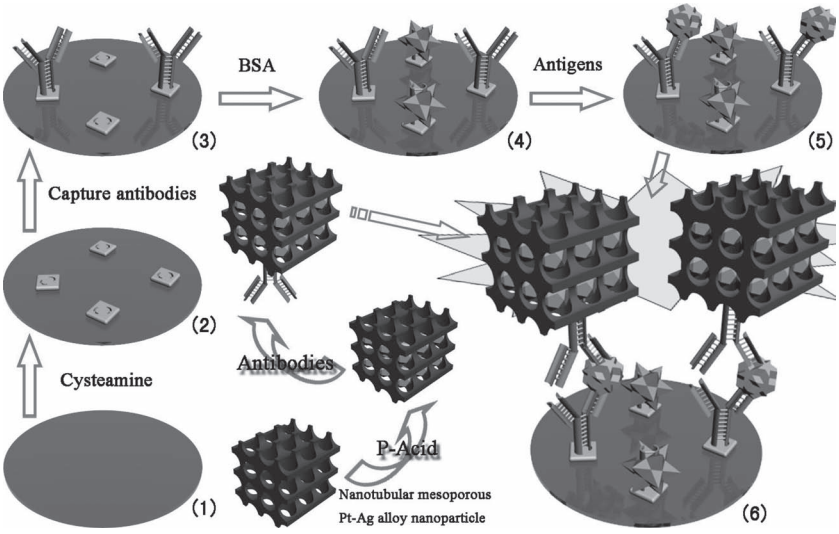

Scheme 2. Schematic representation of fabrication and the assay procedures of this ECL immunosensors on Au working electrode: 1) bare Au working electrode; 2)cysteamine-activated Au working electrode; 3)capture-antibodies-immobilized Au working electrode; 4)BSA-blocked Au working electrode; 5) Au working electrode after incubation with antigen solution; and 6) Au working electrode after incubation with signal antibodies and triggering ECL reaction in the presence of TPrA.

Fabrication of the ECL Immunosensor: As shown in **Scheme 2**, the immunosensor was constructed by immobilizing capture antibodies on the Au working electrodes through CDI cross-linking. Firstly, the Au working electrodes was pretreated before modification by polishing its surface with successively finer grade sand papers and then polished to a mirror smoothness with aqueous slurries of alumina powders (average particle diameters: 0.3 and 0.05 μm Al_2O_3) on a polishing silk. The Au working electrodes was thoroughly rinsed with water and then sonicated in ethanol and ultrapure water in turn.

Then, the washed Au working electrode was immersed in the 3 mM cysteamine solution for 1 h to obtain an amino-groups-modified Au working electrode. After that it was rinsed thoroughly with water and dried under a stream of N_2. After activating by immersing into 3 mM CDI solution for 1 h and washing with buffer, 5 μL of 0.5 mg mL^{-1} anti-CEA capture antibodies were dropped onto the Au working electrode, and reacted at room temperature for 1 h. Subsequently, excess antibodies were washed out with washing buffer. A drop of 5 μL of blocking buffer was dropped on the Au working electrode and incubated for 1 h at room temperature to block possible remaining active sites against nonspecific adsorption. After another washing with buffer the resulting immunosensor was obtained and stored at 4 °C before use.

Analytical Procedure: To carry out the immunoreaction and ECL measurements, the immunosensor was first incubated with a 5 μL drop of CEA standard solutions or serum samples for 50 min at room temperature, followed by washing with buffer. It was then immersed into the solution of signal antibodies for 50 min at room temperature, followed by thoroughly washing with the same buffer to remove unbound signal antibodies. Before and after the incubation, the ECL responses of this immunosensor were both recorded in 0.1 M PBS (pH 7.4) on a luminescence analyzer (IFFM-E, Xi'an Remex Electronic Instrument High-Tech Ltd., Xi'an, China). The scan potential in the range of 0–1.0 V was applied with a scan rate of 0.1 V s^{-1}, and the voltage of the PMT was set at 800 V. ECL signals related to the CEA concentrations could be measured.

Characterization: ^{1}H NMR spectra were obtained on a Varian Inova (400 MHz) spectrometer. Transmission electron microscopy (TEM) images were obtained with a JEM-2010 high-resolution TEM system (JEOL, Japan) opened at an accelerating voltage of 200 kV. Scanning electron microscopy (SEM) images were obtained using a JSM-7401 field emission SEM system (JEOL, Japan). UV-vis experiments were performed with a UV-3900 spectrophotometer (Hitachi, Japan). Emission spectra were obtained with a Fluorolog spectrofluorometer. Electrochemical characterizations of P-acid were made with a CH instruments 600 voltammetric analyzer. A conventional three-electrode setup was used. Au electrode served as the working electrode; an Ag/AgCl (saturated KCl) reference electrode was used for all measurements; a platinum wire was used as a counter electrode. The electrochemistry of P-acid was studied using cyclic voltammetry potential scans in 0.1 M pH 7.4 PBS containing 0.1 M KCl and 1 mM P-acid.

Supporting Information

Supporting Information is available from the Wiley Online Library or from the author.

Acknowledgements

This work was financially supported by the Natural Science Research Foundation of China (21175058 and 51003039), the Technology Development Plan of Shandong Province, China (Grant No. 2011GGB01153) and the Natural Science Foundation of Shandong Province, China (ZR2011BQ019).

Received: February 24, 2012
Published online: June 4, 2012

[1] J. Chen, M. A. Reed, A. M. Rawlett, J. M. Tour, *Science* **1999**, *286*, 1550.
[2] F.-R. F. Fan, J. Yang, S. M. Dirk, D. W. Price, D. Kosynkin, J. M. Tour, A. J. Bard, *J. Am. Chem. Soc.* **2001**, *123*, 2454.
[3] F.-R. F. Fan, R. Y. Lai, J. Cornil, Y. Karzazi, J.-L. Brédas, L. Cai, L. Cheng, Y. Yao, D. W. Price, S. M. Dirk, J. M. Tour, A. J. Bard, *J. Am. Chem. Soc.* **2004**, *126*, 2568.
[4] H. Li, D. R. Powell, R. K. Hayashi, R. West, *Macromolecules* **1998**, *31*, 52.
[5] Q. Zhou, T. M. Swager, *J. Am. Chem. Soc.* **1995**, *117*, 12593.
[6] Q. Zhou, T. M. Swager, *J. Am. Chem. Soc.* **1995**, *117*, 7017.
[7] J.-S. Yang, T. M. Swager, *J. Am. Chem. Soc.* **1998**, *120*, 5321.
[8] J.-S. Yang, T. M. Swager, *J. Am. Chem. Soc.* **1998**, *120*, 11864.
[9] D. T. McQuade, A. E. Pullen, T. M. Swager, *Chem. Rev.* **2000**, *100*, 2537.
[10] T. Ogoshi, Y. Takashima, H. Yamaguchi, A. Harada, *Chem. Commun.* **2006**, 3702.
[11] Z. Chen, C. Xue, W. Shi, F.-T. Luo, S. Green, J. Chen, H. Liu, *Anal. Chem.* **2004**, *76*, 6513.
[12] M. M. Richter, *Chem. Rev.* **2004**, *104*, 3003.
[13] B. D. Muegge, M. M. Richter, *Anal. Chem.* **2003**, *76*, 73.
[14] D. Bruce, M. M. Richter, *Anal. Chem.* **2002**, *74*, 1340.
[15] B. D. Muegge, S. Brooks, M. M. Richter, *Anal. Chem.* **2003**, *75*, 1102.
[16] D. Bruce, M. M. Richter, K. J. Brewer, *Anal. Chem.* **2002**, *74*, 3157.
[17] H. Wei, J. Yin, E. Wang, *Anal. Chem.* **2008**, *80*, 5635.
[18] R. J. Forster, C. F. Hogan, *Anal. Chem.* **2000**, *72*, 5576.
[19] H. Cui, Y. Xu, Z.-F. Zhang, *Anal. Chem.* **2004**, *76*, 4002.
[20] R. Wilson, C. Clavering, A. Hutchinson, *Anal. Chem.* **2003**, *75*, 4244.
[21] D. Asil, A. Cihaner, F. Algı, A. M. Onal, *Electroanalysis* **2010**, *22*, 2254.
[22] G. Jie, L. Wang, J. Yuan, S. Zhang, *Anal. Chem.* **2011**, *83*, 3873.
[23] L. Li, H. Liu, Y. Shen, J. Zhang, J.-J. Zhu, *Anal. Chem.* **2011**, *83*, 661.
[24] H. Jiang, H. Ju, *Anal. Chem.* **2007**, *79*, 6690.
[25] G. Jie, B. Liu, H. Pan, J.-J. Zhu, H.-Y. Chen, *Anal. Chem.* **2007**, *79*, 5574.
[26] S. K. Lee, M. M. Richter, L. Strekowski, A. J. Bard, *Anal. Chem.* **1997**, *69*, 4126.
[27] M. Oyama, S. Okazaki, *Anal. Chem.* **1998**, *70*, 5079.
[28] C. Xu, Y. Li, F. Tian, Y. Ding, *ChemPhysChem* **2010**, *11*, 3320.
[29] C. Xu, Y. Liu, F. Su, A. Liu, H. Qiu, *Biosens. Bioelectron.* **2011**, *27*, 160.
[30] H. Cui, G.-Z. Zou, X.-Q. Lin, *Anal. Chem.* **2003**, *75*, 324.
[31] A. B. Sproul, M. A. Green, *J. Appl. Phys.* **1991**, *70*, 846.
[32] S. K. Poznyak, D. V. Talapin, E. V. Shevchenko, H. Weller, *Nano Lett.* **2004**, *4*, 693.
[33] Y.-M. Fang, J.-J. Sun, A.-H. Wu, X.-L. Su, G.-N. Chen, *Langmuir* **2008**, *25*, 555.
[34] G.-L. Wang, P.-P. Yu, J.-J. Xu, H.-Y. Chen, *J. Phys. Chem. C* **2009**, *113*, 11142.
[35] S. Mandal, D. Roy, R. V. Chaudhari, M. Sastry, *Chem. Mater.* **2004**, *16*, 3714.
[36] G. T. Hermanson, *Bioconjugate Techniques*, 2nd ed., Academic Press Inc, Rockford, IL **2008**, pp. 228–231.